

## Electron spin resonance study of a $\text{La}_{0.7}\text{Ca}_{0.3}\text{MnO}_3$ single crystal

This article has been downloaded from IOPscience. Please scroll down to see the full text article.

2003 J. Phys.: Condens. Matter 15 4161

(<http://iopscience.iop.org/0953-8984/15/24/310>)

View [the table of contents for this issue](#), or go to the [journal homepage](#) for more

Download details:

IP Address: 171.66.16.121

The article was downloaded on 19/05/2010 at 12:18

Please note that [terms and conditions apply](#).

# Electron spin resonance study of a $\text{La}_{0.7}\text{Ca}_{0.3}\text{MnO}_3$ single crystal

Keon Woo Joh<sup>1</sup>, Chang Hoon Lee<sup>1</sup>, Cheol Eui Lee<sup>1,4</sup>, N H Hur<sup>2</sup> and H-C Ri<sup>3</sup>

<sup>1</sup> Department of Physics and Institute for Nano Science, Korea University, Seoul 136-701, Korea

<sup>2</sup> Korea Research Institute of Standards and Science, Taejon 305-600, Korea

<sup>3</sup> Korea Basic Science Institute, Taejon 305-333, Korea

E-mail: rscel@korea.ac.kr (Cheol Eui Lee)

Received 13 November 2002, in final form 6 May 2003

Published 6 June 2003

Online at [stacks.iop.org/JPhysCM/15/4161](http://stacks.iop.org/JPhysCM/15/4161)

## Abstract

Comprehensive measurements of electron spin resonance were carried out on a  $\text{La}_{0.7}\text{Ca}_{0.3}\text{MnO}_3$  single crystal over a wide temperature range covering the ferromagnetic as well as the paramagnetic phases. Our analysis of the asymmetric lineshapes indicates that the phase segregation of good and poor conducting regions persists far above the ferromagnetic–paramagnetic phase transition temperature.

(Some figures in this article are in colour only in the electronic version)

## 1. Introduction

Perovskite manganites with mixed manganese valence,  $\text{La}_{1-x}\text{D}_x\text{MnO}_3$  with D a divalent metal, have attracted a great deal of attention due to the anomalously large negative ‘colossal’ magnetoresistance (CMR) for  $0.2 < x < 0.5$  [1–5]. In this composition range, the system shows the simultaneous appearance of metallic conduction and ferromagnetism at low temperatures while the end materials ( $x = 0, 1$ ) are insulating antiferromagnets. The underlying physics of this system has been traditionally explained in terms of the double-exchange (DE) mechanism due to Zener [6–8]; however, recent works have shown that the DE alone may not be sufficient to explain the phenomenon. Other effects such as lattice polarons due to the Jahn–Teller (JT) distortion [9], magnetic polarons, and electron localization [10] were advanced as additional physical effects. One interesting proposal is that the phase separation (PS) of carriers, already seen in other systems [11], is an essential ingredient in understanding the CMR materials [12].

<sup>4</sup> Author to whom any correspondence should be addressed.

Several computational works indicated that a homogeneous state is unstable against PS, as charge carriers are doped into the manganites [13–15]. It was also shown that the inclusion of Coulomb interactions leads to a charge-inhomogeneous state with clusters of one phase (high carrier density) embedded in the other (low carrier density). Since an inhomogeneity in the carrier density also gives rise to a corresponding inhomogeneity in the magnetic structures, the PS state consists of ferromagnetic metallic clusters surrounded by either antiferromagnetic regions or paramagnetic insulators [12]. Thus, a detailed microscopic study of the magnetic properties of perovskite manganites will shed light on the PS model. Currently, evidence for the inhomogeneous nature of perovskite manganites is offered by several studies, including scanning tunnelling spectroscopy, x-ray absorption, neutron scattering, and NMR investigations [16–20]. However, as it turns out, the electron spin resonance (ESR) method, which directly probes the electron spins, can also be useful for this purpose. Several ESR studies have already been carried out [21–25], and spin clusters in an inhomogeneous nature for the doped manganites have been proposed by some ESR work [26–28]. Up to now, most of the ESR studies have been carried out on powders or thin-film samples, as a sample dimension greater than the skin depth at the microwave frequency gives rise to asymmetric ESR lineshapes [29, 30]. While the absolute values of  $g_{eff}$  and the linewidth may be less reliable, the asymmetric lineshape can give more information on the inhomogeneity of the sample [30].

Rettory *et al* and Ivanshin *et al* have performed an ESR experiment on a  $\text{La}_{0.7}\text{Ca}_{0.3}\text{MnO}_3$  (LCMO) and a  $\text{La}_{1-x}\text{Sr}_x\text{MnO}_3$  single-crystal sample with dimensions larger than the skin depth at the microwave frequency, and obtained asymmetric lineshapes [23]. However, they did not fully discuss the asymmetry of the lineshape. While Ivanshin *et al* discussed the temperature dependence of the dispersion-to-absorption ratio, similar to the positive-peak-to-negative-peak ratio in differential ESR absorption, they did not discuss the microscopic inhomogeneity of the sample due to the small sample size, for which change of the dispersion-to-absorption ratio arises only from the change of the macroscopic resistance. In order to carefully examine the local magnetic properties related to the inhomogeneous nature of the CMR systems, we have made ESR measurements and carried out a quantitative analysis for a single-crystal sample of LCMO with dimensions larger than the microwave skin depth, covering a wide temperature range both above and below the magnetic transition temperature ( $T_c$ ).

## 2. Experiment

An LCMO single-crystal sample was prepared by the floating zone method. The oxygen content of the sample was determined by iodometric titration: it was estimated to be about  $2.99 \pm 0.01$ , assuming an ideal La/Ca ratio of  $x = 0.3$ . The resistivity was measured by the standard four-probe method, and the dc magnetization was measured with a superconducting quantum interference device (SQUID) magnetometer. The magnetic ordering temperature is conventionally defined to be that of the onset of the ferromagnetic magnetization, which gave the  $T_c$ -value of 229 K, in good agreement with the conductivity measurements. The sample was ball-milled into a spherical shape with a diameter of about 0.1 mm in order to exclude orientation dependence, in a macroscopic sense. The rotation pattern of the crystal was also obtained, but there was no spectral change in position or form, indicating that there is no anisotropy at the atomic level. The sample dimensions were greater than the calculated skin depth at the resistive peak temperature, and the ESR measurements were made at 9.4 GHz employing a Bruker ESP 300E spectrometer using a microwave power of 1 mW and a modulation amplitude of 5 G.

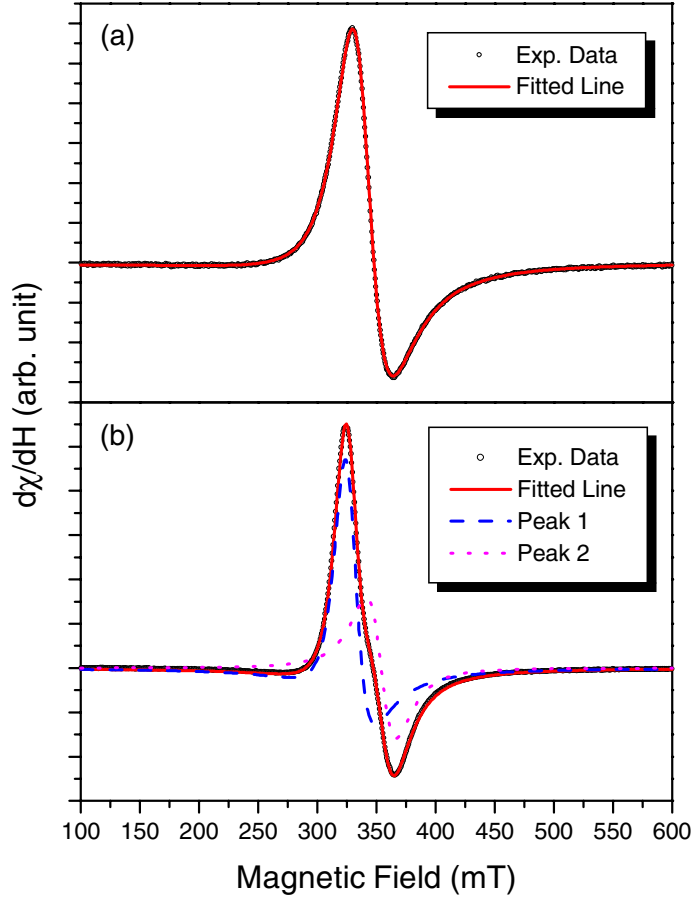


Figure 1. Typical differential ESR spectra (a) above  $T_c$  (300 K) and (b) below  $T_c$  (163 K).

### 3. Results and discussion

The differential ESR spectra for our sample are shown in figure 1. As can be seen, the ESR spectra have an asymmetric lineshape, which is usually expected in metallic samples. The asymmetric Dysonian lineshape is a mixture of absorptive and dispersive susceptibilities [29, 30]. The spectra were well fitted by the formula suggested by Peter *et al* [31]:

$$\frac{dP}{dH} \propto \frac{d}{dH} \left( \frac{\Delta H + \alpha(H - H_0)}{(H - H_0)^2 + \delta H^2} + \frac{\Delta H + \alpha(H + H_0)}{(H + H_0)^2 + \delta H^2} \right), \quad (1)$$

where  $\alpha$  is the ratio of the dispersive part to the absorptive part. While the ESR spectra far above  $T_c$  are well fitted by one Dysonian line, as shown in figure 1(a), the ESR spectra at low temperatures are well fitted only by using two Dysonian lines, peak 1 and peak 2.

In general, the asymmetry parameter  $\alpha$  is related to  $d/\delta$  where  $d$  is the sample dimension and  $\delta$  is the skin depth. The classical skin depth is given by

$$\delta = \sqrt{\rho/\mu_0\omega}, \quad (2)$$

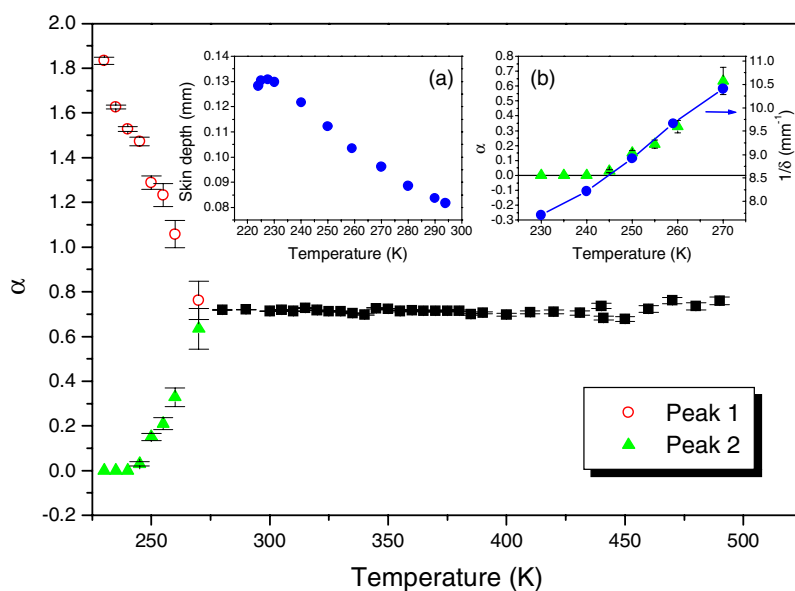


**Figure 2.** The temperature dependence of the parameter  $\alpha$ , the ratio of the dispersive part to the absorptive part of the ESR spectrum. Open circles: the parameter  $\alpha$  for peak 1. Solid triangles: the parameter  $\alpha$  for peak 2. Inset (a): the solid circles indicate the temperature dependence of the skin depth, calculated using equation (2) from experimental data. Inset (b): the relationship between the skin depth and the parameter  $\alpha$  for peak 2. Solid circles: the inverse of the skin depth in inset (b). Solid triangles: the parameter  $\alpha$  for peak 2.

where  $\rho$  is the resistivity and  $\omega$  is the microwave frequency. Thus, an increase in the resistivity of the sample is expected to result in a decrease of  $\alpha$ . However, as can be seen in figure 2, above the temperature of 270 K, which is well above the  $T_c$ , the parameter  $\alpha$ , obtained from spectral fitting of the ESR data, is almost temperature independent, which can generally be taken to indicate that the electrical conduction is limited by the phonon scattering [32]. Below 270 K, for one of the peaks  $\alpha$  decreases with decreasing temperature, whereas for the other peak it increases with decreasing temperature. As shown in the inset (b) of figure 2, the parameter  $\alpha$  for peak 2 closely follows the (inverse) skin depth dependence. It is worthwhile noting that below about 245 K, the skin depth becomes sufficiently greater than the sample size of about 0.1 mm, and the parameter  $\alpha$  for peak 2 becomes 0, corresponding to the simple Lorentzian lineshape. In figure 2, while peak 2 follows the normal behaviour of the (inverse) skin depth dependence, the temperature dependence of  $\alpha$  for peak 1 shows an opposite skin depth dependence, an anomalous behaviour that cannot be explained by the normal skin depth effect.

In figure 3(a) we display the temperature dependence of the resonance fields ( $H_0$ ). The resonance field for peak 1 decreases with decreasing temperature, whereas that for peak 2 increases with decreasing temperature. This indicates that two different kinds of spin contribute to the microwave absorption. The EPR intensities of the two EPR peaks as well as the total EPR intensity are shown in figure 4 as a function of temperature. While the EPR intensities are well separated at low temperatures, it is hard to assign absolute meaning to the EPR intensities as the microwave cannot penetrate into the whole volume of the sample and the penetration depth changes as a function of temperature.

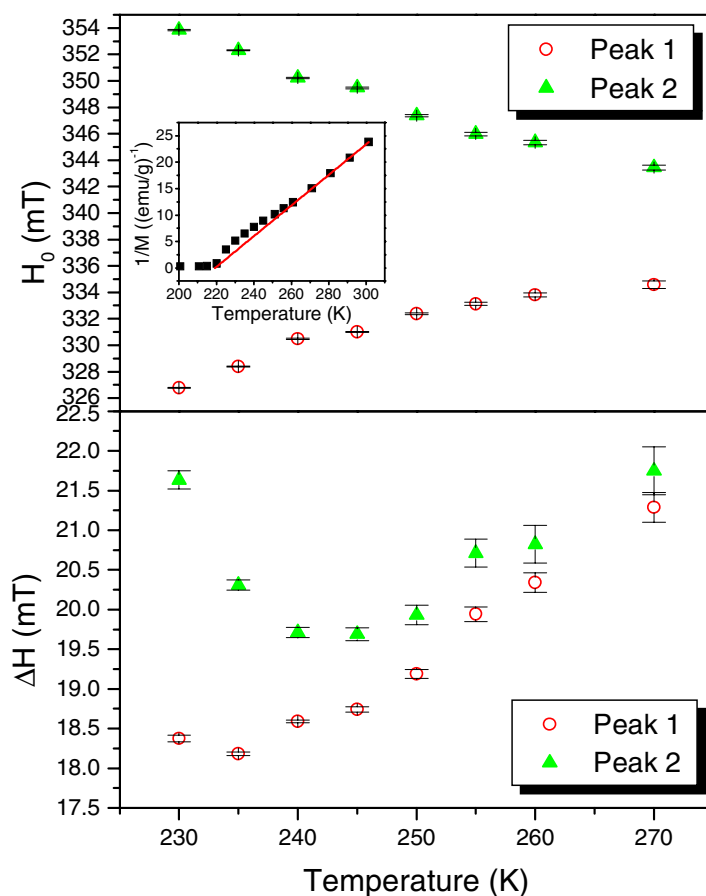


**Figure 3.** Temperature dependences of the resonance field and the linewidth for peaks 1 and 2. Inset: the temperature dependence of the inverse magnetization. The solid line indicates the high-temperature extrapolation according to the Curie–Weiss law.

It is generally known that ESR signals arise from both  $\text{Mn}^{3+}$  ions and  $\text{Mn}^{4+}$  ions, but due to the DE interaction, the ESR absorptions for  $\text{Mn}^{3+}$  ions and  $\text{Mn}^{4+}$  ions cannot be resolved into two distinct lineshapes, which is the bottleneck effect [22]: the difference of the two resonance fields is smaller than the linewidth. In our case, if the difference of the two resonance fields is larger than half the linewidth, the two peaks can be resolved because the lineshape is asymmetric. One possible explanation for our measurements is the formation of ferromagnetic droplets above  $T_c$ . When the ferromagnetic droplets are formed, the resonance field due to the spins in the ferromagnetic droplets decreases with decreasing temperature due to the ferromagnetic exchange interaction, whereas that for the spins in the paramagnetic background increases with decreasing temperature due to the demagnetization field from the ferromagnetic droplets.

In summary, we have studied the nature of spin systems in a LCMO single crystal exhibiting CMR by means of ESR measurements. Our data provided convincing experimental microscopic evidence for the applicability of the PS model, and revealed the detailed magnetic structure of the ferromagnetic microregions surrounded by insulating regions both above and below  $T_c$ .

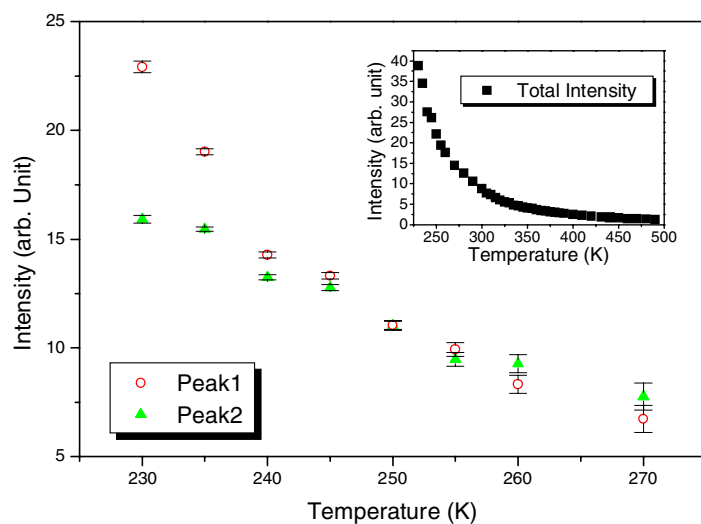


**Figure 4.** Temperature dependences of the EPR intensities for peaks 1 and 2. Inset: the temperature dependence of the total EPR intensity.

## Acknowledgments

This work was supported by the KISTEP (National Research Laboratory and Proton Engineering R&D Project No M102KS010001-02K1901-01810). Measurements at the Korea Basic Science Institute (KBSI), Seoul, are acknowledged.

## References

- [1] Jin S, Tiefel T H, McCormack M, Fastnacht R A, Ramesh R and Chen L H 1994 *Science* **264** 413
- [2] McCormack M, Jin S, Tiefel T H, Fleming R M, Phillips J M and Ramesh R 1994 *Appl. Phys. Lett.* **64** 3045
- [3] Schieffer P, Ramirez A P, Bao W and Cheong S-W 1995 *Phys. Rev. Lett.* **75** 3336
- [4] Hwang H Y, Cheong S-W, Radaelli P G, Marezio M and Batlogg B 1995 *Phys. Rev. Lett.* **75** 914
- [5] Hundley M F, Hawley M, Heffner R H, Jia Q X, Neumeier J J, Tesmer J, Thompson J D and Wu X D 1995 *Appl. Phys. Lett.* **67** 860
- [6] Zener C 1951 *Phys. Rev.* **81** 440
- [7] Anderson P W and Hasegawa H 1955 *Phys. Rev.* **100** 615
- [8] de Gennes P-G 1960 *Phys. Rev. Lett.* **118** 141
- [9] Millis A J, Littlewood P B and Shraiman B I 1995 *Phys. Rev. Lett.* **74** 5144
- [10] Varma C M 1996 *Phys. Rev. B* **54** 7328
- [11] Nagaev E L 1995 *Sov. Phys.-Usp.* **38** 497
- [12] Moreo A, Yunoki S and Dagotto E 1999 *Science* **283** 2034
- [13] Yunoki S, Hu J, Malvezzi A L, Moreo A, Furukawa N and Dagotto E 1998 *Phys. Rev. Lett.* **80** 845
- [14] Yunoki S, Moreo A and Dagotto E 1998 *Phys. Rev. Lett.* **81** 5612
- [15] Shen S-Q and Wang Z D 1998 *Phys. Rev. B* **58** R8877
- [16] Fäth M, Freisem S, Menovsky A A, Tomioka Y, Aarts J and Mydosh J A 1999 *Science* **285** 1540
- [17] Booth C H, Bridges F, Kwei G H, Lawrence J M, Cornelius A L and Neumeier J J 1998 *Phys. Rev. B* **57** 10440
- [18] Lynn J W, Erwin R W, Borchers J A, Huang Q, Santoro A, Peng J-L and Li Z Y 1996 *Phys. Rev. Lett.* **76** 4046
- [19] De Teresa J M, Ibarra M R, Algarabel P A, Ritter C, Marquina C, Blasco J, Garcia J, del Moral A and Arnold Z 1997 *Nature* **386** 256
- [20] Allodi G, De Renzi R, Guidi G, Licci F and Pieper M W 1997 *Phys. Rev. B* **56** 6036
- [21] Oseroff S B, Torikachvili M, Singley J, Ali S, Cheong S-W and Schultz S 1996 *Phys. Rev. B* **53** 6521
- [22] Shengelaya A, Zhao G-M, Keller H and Müller K A 1996 *Phys. Rev. Lett.* **77** 5296

- 
- [23] Rettory C, Rao D, Singley J, Kidwell D, Oseroff S B, Causa M T, Neumeier J J, McClellan K J, Cheong S-W and Schultz S 1998 *Phys. Rev. B* **58** 14490
- [24] Shengelaya A, Zhao G-M, Keller H, Müller K A and Kochelaev B I 2000 *Phys. Rev. B* **61** 5888  
Ivanshin V A, Deisenhofer J, Krug von Nidda H-A, Loidl A, Mukhin A A, Balbashov A M and Eremin M V  
2000 *Phys. Rev. B* **61** 6213
- [25] Li G, Zhou H-D, Feng S-J and Li Z-G 2002 *J. Phys.: Condens. Matter* **14** 211
- [26] Lofland S E, Bhagat S M, Kwon C, Tyagi S D, Mukovskii Y M, Karabashev S G and Balbashov A M 1997  
*J. Appl. Phys.* **81** 5737
- [27] Causa M T, Tovar M, Caneiro A, Prado F, Ibañez G, Ramos C A, Butera A, Alascio B, Obradors X, Piñel S,  
Rivadulla F, Vázquez-Vázquez C, López-Quintela M A, Rivas J, Tokura Y and Oseroff S B 1998 *Phys. Rev.*  
**B 58** 3233
- [28] Chauvet O, Goglio G, Molinie P, Corraze B and Brohan L 1998 *Phys. Rev. Lett.* **81** 1102
- [29] Dyson F J 1955 *Phys. Rev.* **98** 349
- [30] Feher G and Kip A F 1955 *Phys. Rev.* **98** 337
- [31] Peter M, Shaltier D, Wernick J H, Williams H J, Mock J B and Sherwood R C 1962 *Phys. Rev.* **126** 1395
- [32] Aubay E and Gourier D 1993 *Phys. Rev. B* **47** 15023